Protocol for Evaluating Anion Exchange Membranes for Nonaqueous Redox Flow Batteries

Jessica L. Tami,[a] Md. Motiur R. Mazumder,[b,d] Grace E. Cook,[a] Shelley D. Minteer,[b,d*] and Anne J. McNeil[a,c,*]

[a] Department of Chemistry, University of Michigan, Ann Arbor, Michigan, 48109-1055, United States.

[b] Department of Chemistry, Missouri University of Science and Technology, Rolla, Missouri, 65409-6518, United States.

[c] Macromolecular Science and Engineering Program, University of Michigan, Ann Arbor, Michigan, 48109-1055, United States.

[d] Kummer Institute Center for Resource Sustainability, Missouri University of Science and Technology, Rolla, Missouri, 65409-6518, United States.

Keywords: Anion exchange membranes, redox flow batteries, crossover

ABSTRACT: Nonaqueous redox flow batteries (NARFBs) often suffer from reduced battery lifetime and decreased coulombic efficiency due to crossover of the redox-active species through the membrane. One method to mitigate this undesired crossover is to judiciously choose a membrane based on several criteria: swelling and structural integrity, size and charge(s) of redox active species, and ionic conductivity. Most research to date has focused on reducing crossover by synthesizing modified redox-active molecules and/or new membranes. However, no standard protocol exists to compare membranes and a comprehensive study comparing membranes has yet to be done. To address both these limitations, we evaluate herein 26 commercial anion exchange membranes (AEMs) to assess their compatibility with common nonaqueous solvents and their resistance to crossover by using neutral and cationic redox-active molecules. Ultimately, we found that all the evaluated AEMs perform poorly in organic solvents due to uncontrolled swelling, low ionic conductivity, and/or high crossover rates. We believe that this method, and the generated data, will be useful to evaluate and compare the performance of all anion exchange membranes—commercial and newly synthesized—and should be implemented as a standard protocol for all future work.

INTRODUCTION

Renewable energy can be harvested through several avenues, including solar panels and wind turbines. However, solar and wind energy are intermittent, meaning they are not continuously accessible.[1] A safe, sustainable, and efficient way to store renewable energy is necessary so that it can be employed when needed. A promising technology for energy storage is the redox flow battery (RFB), which has the potential to be used in grid-scale operations.[2] RFBs consist of an electrochemical flow cell and two reservoirs, one of which contains an anolyte (redox-active species that undergoes reduction upon charging) and the other a catholyte (redox-active species that undergoes oxidation upon charging), both dissolved in a solvent with a supporting electrolyte (Scheme 1A).[3] An advantage to RFBs is that power and capacity can be independently scaled. Power is affected by the size of the electrodes (in each cell) and the number of cells whereas capacity is affected by the volume and concentration of redox-active molecules in the reservoirs.[4] The state-of-the-art commercial RFB is aqueous and uses expensive vanadium compounds for the redox-active molecules and hazardous sulfuric acid for the supporting electrolyte.[5,6,7] Additionally, aqueous batteries have a relatively small thermodynamic window (1.23V) due to the hydrogen evolution reaction in reducing environments and the oxygen evolution reaction in oxidizing environments.[8] In contrast, nonaqueous redox flow batteries (NARFBs) have a larger operating potential window (e.g., ~5V in acetonitrile), increasing the possibilities of redox-active molecules, and enabling higher power densities as a result of larger attainable open circuit voltages (OCV).[9]

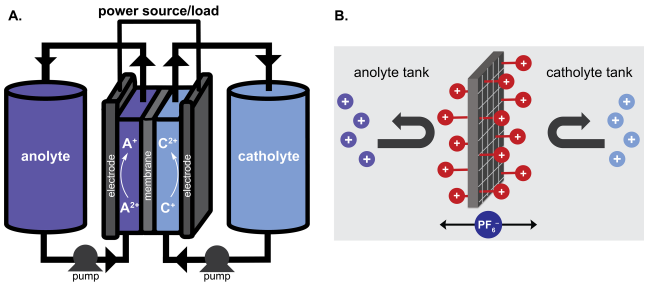

Scheme 1. (A) Redox flow battery where A stands for anolyte (the redox-active species that undergoes reduction upon charging), and C stands for catholyte (the redox-active

species that undergoes oxidation upon charging). (B) Anion exchange membrane impeding positively charged redox-active species from crossing over.

Between the two electrodes in a flow battery is a membrane or a separator, that functions to isolate the anolyte from the catholyte, preventing crossover of redox-active molecules.[10] Several membrane types have been used in RFBs, including polymers of intrinsic microporosity (PIMs), porous separators, ion-exchange membranes, and ceramic membranes.[11] Each type of membrane or separator caters to a specific system. For example, PIMs offer size exclusion, which is advantageous when working with oligomeric or polymeric redox-active materials.[12,13] Porous separators such as Daramic® or Celgard®, have been frequently used in NARFBs due to their relatively high ionic conductivity, which enables battery cycling at higher current densities.[14,15,16] However, this improved conductivity comes at the expense of high crossover rates, especially with small redox-active species. The result is lower coulombic efficiencies and lifetimes of the battery. One method to decrease crossover is to use a pre-mixed flow cell wherein equal quantities of anolyte and catholyte are dissolved in each reservoir[17,18], but doing so effectively wastes half of the redox-active materials. Additionally, there will still be a concentration gradient of the charged species across the cell during cycling, so crossover may still occur, and coulombic efficiency will suffer. A technologically relevant battery (i.e., a battery with high capacity, energy density, and energy efficiency) will be non-symmetric and have a membrane that is both highly conductive and prevents crossover.

Commercial ion-exchange membranes were originally fabricated for aqueous systems, such as fuel cells, water purification, desalination, dialysis, and/or aqueous RFBs.[19,20,21] Specifically, anion exchange membranes (AEMs) are cross-linked polymers, assembled into three-dimensional networks with fixed, ionic functional groups (i.e., $-NH_3^+$, $-NRH_2^+$, $-NR_2H^+$, $-NR_3^+$, and $-SR_2^+$).[19] AEMs should repel positively charged molecules, with a higher repulsion resulting from a more charge-dense molecule, ensuring that cationic molecules stay in their respective tank. In AEMs, only anionic supporting electrolyte ions, like PF_6^- or BF_4^-, can traverse the membrane for charge balancing during charging and discharging (Scheme 1B). AEMs have been used in nonaqueous, inorganic redox flow batteries for decades[22,23,24,25] but have more recently been adopted in nonaqueous organic redox flow batteries. For instance, Sanford and coworkers used an AEM in organic NARFBs (Fumasep FAP-375-PP) to mitigate the crossover of redox-active cyclopropenium species.[12,26,27,28] Increasing charge incorporation and molecular size decreased the rate of crossover, with a tetramer (4^+ charge) crossing over so slowly it was below the limit of detection within the timeframe of their experiment. As a result, FAP-375-PP has been the go-to commercial membrane in many nonaqueous redox flow battery studies,[29,30,31,32] enabling non-symmetric small-molecule batteries. However, FAP-375-PP has recently been discontinued by the manufacturer.

To date, a systematic study has not directly compared AEMs,[29,33,34,35,36,37,38] so it is unclear what membranes would perform best in specific flow battery systems. To address this limitation, we evaluated herein 26 AEMs (Table 1) for structural stability in electrochemically relevant organic solvents. From these results, seven membranes were selected for further evaluation, including measuring ionic conductivities, crossover rates, and their performance in a redox flow battery. Overall, these data reveal that most commercial AEMs do not perform satisfactorily in lab-scale NARFBs. Moving forward, we suggest that researchers developing new membranes and/or evaluating new commercial membranes utilize the standard protocol described herein for benchmarking and comparison.

Table 1. Commercial anion exchange membranes evaluated. Blocks of color indicate different manufacturers of AEMs.

Fumasep		Sustainion
FAP-330	FAB-PK-130	E30-50, T
FAPQ-330	FAD-55	E28-50, T
FAP-450	FAS-30	B22-50, T
FAA-3-30	FAS-50	X37-50, RT
FAA-3-50	FAP-330-PE	X37-50, T
FAPQ-375-PP	FAD-PET-75	**PiperION**
FAA-3-PK-75	FAS-PET-75	15 μm PTFE
FAA-3-PK-130	**AMI-7001S**	20 μm
FAM	**AEMION+**	80 μm

RESULTS AND DISCUSSION

Most commercial anion exchange membranes dissolve or deform in nonaqueous solvents. To qualitatively assess the membrane's structural stability, the AEMs were examined after soaking in neat organic solvent for 48 h to simulate long-term cycling conditions. Before this experiment, all membranes were pre-treated in a saturated, aqueous solution of potassium hexafluorophosphate (KPF_6) to exchange the mobile counterions in the polymer resin with PF_6^- anions to match the supporting electrolyte used in crossover and battery studies. Upon pre-treatment and subsequent drying, the membranes were cut into small rectangles and submerged in MeCN, PC, DMF, DMA, and DME, separately. Every membrane deformed in DMF and DMA, either dissolving completely or swelling excessively after soaking. Too much swelling will immediately allow redox species to crossover the membrane.[11,39] Many membranes remained intact in DME, but some turned opaque, which is likely caused by a change in polymer properties (e.g., solubility). Photos of all ion-exchanged AEMs, before and after soaking in organic solvents, are included in the supporting information (SI section III). Due to the incompatibility of AEMs in DMF and DMA, and the high relative permittivity of DME, we chose MeCN and PC as the organic solvents for subsequent studies.[40] Additionally, PC and MeCN are the two most widely used solvents in the NARFB field. Acetonitrile is an ideal organic solvent in NARFBs because of its large electrochemical window and high dielectric permittivity. Propylene carbonate is considered a green solvent because of its low relative toxicity and environmental impact, making it attractive for commercial applications.[41] However, PC does

have some drawbacks, such as a higher viscosity and lower conductivity than comparable electrolytes in MeCN. Among the 26 commercial anion exchange membranes examined, only seven demonstrated stability (no dissolution or deformation) in MeCN and PC: FAP-330, FAPQ-330, FAP-450, FAPQ-375-PP, FAP-330-PE, FAM, and AMI-7001S. These membranes were chosen for further testing.

High weight increases from membrane swelling lead to higher permeability. Next, crossover rates were measured for three different redox-active small molecules with increasing positive charges: neutral ferrocene (Fc, catholyte), monocationic (1^+) ammonium-appended ferrocene ($FcNPF_6$, catholyte), and dicationic (2^+) butyl viologen ($BuV2PF_6$, anolyte) (Figure 1A). We chose these molecules because they are electrochemically stable to galvanostatic cycling and are commercially available or easily synthesized. Additionally, these small molecules have similar hydrodynamic radii (molecular size in solution),[42] so conclusions regarding crossover rates can be made primarily based on charge interactions with the positively charged membrane instead of size-exclusion. An H-cell was used for crossover studies,[43] enabling a membrane to sit between two half cells: one, the retentate, is composed of 25 mM redox-active material in supporting electrolyte and solvent (either 0.5 M KPF_6 in MeCN or 0.1 M KPF_6 in PC) and the other, the permeate, only contains supporting electrolyte in solvent (Figure 1B). A lower concentration of supporting electrolyte was used in PC due to the low solubility of KPF_6. Crossover is monitored by cyclic voltammetry, which relates measured peak current to the concentration of redox-active material using a three-electrode set-up on the permeate side of the H-cell. Though not used in this study, ultraviolet-visible (UV-Vis) and nuclear magnetic resonance (NMR) spectroscopy are also viable methods of measuring crossover.[44]

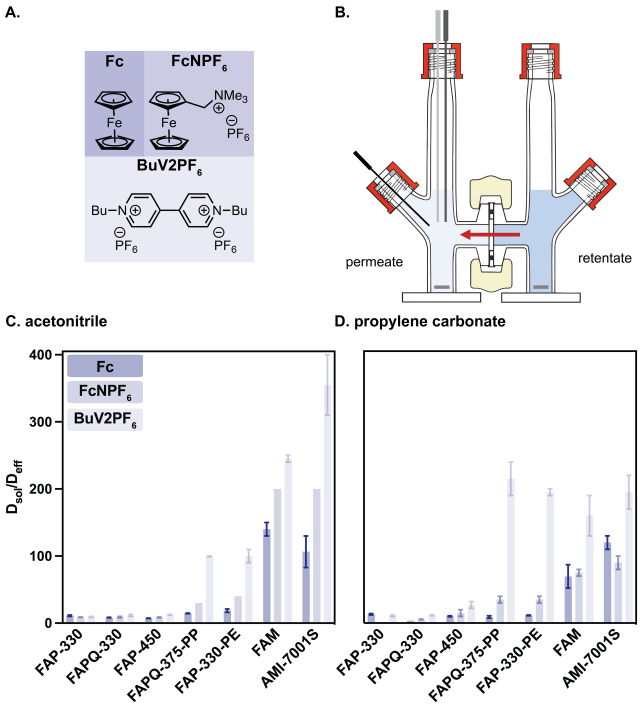

Figure 1. (A) Structures of catholytes and anolyte. (B) H-cell used for crossover experiments, adapted from Adams & Chittenden Scientific Glass Coop.[45] (C) Plot of membrane performance (D_{sol}/D_{eff}) in 0.5 M KPF_6 in MeCN. (D) Plot of membrane performance in 0.1 M KPF_6 in PC. All bars represent the average of two trials. The error bars represent the range of values.

Each membrane has a different thickness (l), and each molecule has a different diffusion coefficient in solution (D_{sol}). To compare between membranes and molecules, we used the ratio between the redox-active molecule's diffusion coefficient in the electrolyte (D_{sol}) and its effective diffusion, or permeability, through the membrane (D_{eff}). Specifically, we used the Randles-Ševčík equation to calculate D_{sol}[46,47] (SI section VII) and the following equation, derived from Fick's laws of diffusion, for D_{eff}[48] (SI section VIII):

$$D_{eff} = \frac{C_{permeate} * l * V_{permeate}}{C_0 * A}$$

$C_{permeate}$ is the initial rate of crossover (mol/s*cm^3), l is the thickness of the membrane (cm), $V_{permeate}$ is the volume of the permeate (cm^3), C_0 is the initial redox material concentration on the retentate side (mol/cm^3), and A is the area of the membrane exposed to solution (cm^2). Both the absolute value and the relative values of D_{sol}/D_{eff} between molecules are important measurements. A higher absolute value of D_{sol}/D_{eff} equates to a better membrane blocking ability, whereas the relative values between the redox-active molecules studied herein reflects the membranes' selectivity for repelling positively charged molecules.[13] We want to highlight that D_{eff} is the product of redox species diffusion through the membrane (transport) and absorption (e.g., partitioning through the membrane), which is a thermodynamic process. Active species transport is important in flow cell cycling and can affect capacity fade, particularly in less conductive membranes, but it is not the sole contributor to permeability.

In MeCN, FAM and AMI-7001S are the best at suppressing crossover of all molecules. Both membranes display ion selectivity because they suppress the dication ($BuV2PF_6$) better than the monocation ($FcNPF_6$) and the monocation better than neutral compound (Fc) (Figure 1C). Though the two AEMs have the slowest rates of crossover, they have low ionic conductivity and require a large overpotential to run in a NARFB (vide infra). In PC, the most ion-selective membranes were FAPQ-375-PP and FAP-330-PE, both of which dramatically suppress the crossover of the dication compared to the monocation and neutral molecule (Figure 1D). These membranes, however, have both been discontinued from commercial suppliers. FAM and AMI-7001S also performed well comparatively but again suffered from low ionic conductivity (vide infra). Permeability (D_{eff}) should be no higher than 10^{-10} cm^2/s and the lowest (slowest) value obtained in this work was 10^{-8} cm^2/s for FAM and AMI-7001S in PC, a factor of 10^2 discrepancy, meaning that even the best performers in our study could never be commercially viable.[39]

Though we cannot attribute performance to the membranes' chemical structure, which is proprietary, we observe a negative correlation between solvent uptake and membrane performance. Membranes with a high (>60%) solvent uptake generally have a smaller D_{sol}/D_{eff} value. For example, the weight of FAP-330 increased by 327% after soaking in MeCN and is a poor membrane with respect to crossover (D_{sol}/D_{eff} of 9.4 for BuV2PF$_6$). In contrast, FAM and AMI-7001S exhibited a more moderate weight increase of 24% and 31%, respectively, and have the best crossover performance (D_{sol}/D_{eff} of 240 and 360 for BuV2PF$_6$, respectively) in MeCN (SI Table S2). Considering the overall poor performance of the selected commercial membranes, better AEMs are needed.

AEMs with the least crossover have the lowest ionic conductivity. In addition to monitoring crossover in H-cells, AEMs should be tested in a flow battery for a more accurate comparison to grid-scale applications. Flow batteries were run using cationic FcNPF$_6$ as the catholyte and dicationic BuV2PF$_6$ as the anolyte, with either 0.5 M KPF$_6$ in MeCN or 0.1 M KPF$_6$ in PC. The battery had a theoretical OCV of 1.05V, which is the difference in voltage between the reduction and oxidation potentials of the anolyte and catholyte. A high ionic conductivity is critical for AEMs in a flow cell to complete the circuit and balance charge efficiently. Ionic conductivity is an intrinsic property of membranes in supporting electrolytes, and, in our study, is measured via electrochemical impedance spectroscopy (EIS), though it could also be measured with a four-point probe.[49] For AEMs in nonaqueous systems, a practical ionic conductivity range is >1 mS/cm by way of the maximum area-specific resistance (ASR) for a membrane with a thickness of ~25 µm (2.3 Ω*cm^2).[50,51] Figure 2A depicts the targeted properties with high ionic conductivity and low redox-active molecule permeability. We observed that the following membranes were in the target ionic conductivity range in MeCN: FAP-330, FAPQ-330, FAP-450, FAPQ-375-PP, and FAP-330-PE. FAM and AMI-7001S had much lower ionic conductivities, most likely due to their thickness. For PC, only FAP-330, FAPQ-330, FAP-450, and FAP-330-PE were in the target ionic conductivity range. When plotting permeability and ionic conductivity, no membrane, solvent, or redox molecule combination was conducive to the overall target performance (Figure 2B). Note that the lower concentration of KPF$_6$ in PC (due to low solubility) compared to MeCN contributes to a lower ionic conductivity under these conditions. When taking our previous crossover data into account, we can conclude that no AEM has an acceptable performance in NARFBs, due to either high permeability, low ionic conductivity, or both.

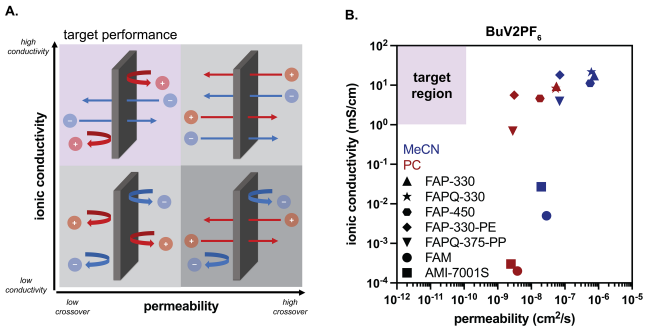

Figure 2. (A) Theoretical depiction of ionic conductivity of supporting electrolyte anions and permeability of redox-active cations through anion exchange membranes. (B) Ionic conductivity and permeability of each AEM in MeCN and PC with BuV2PF$_6$.

Battery testing enables the capacity fade, coulombic efficiency, and voltage efficiency to be measured, among other variables. Capacity fade measures how much redox-active material can be discharged over time, with a lower fade equating to a longer battery lifetime.[52] Coulombic efficiency is the difference between the capacities reached during charging and discharging and reflects how much of stored charge is accessible. Voltage efficiency accounts for any overpotential necessary to run the battery and dictates whether enough power is generated to be commercially viable. Ideally, a battery will have low capacity fade, high coulombic efficiency, and high voltage efficiency. In MeCN, the membranes with the lowest capacity fade and the highest coulombic efficiency were FAM and AMI-7001S (Figure 3). However, both FAM and AMI-7001S have low voltage efficiencies (34% and 21%, respectively) (Table 2), requiring considerably more energy to run the battery than the OCV. In PC, the best membrane was FAP-330-PE, which had the lowest capacity fade of 10% over 22 h (though still impractical for RFBs), with a high coulombic efficiency (97%) and modest voltaic efficiency (80%).[53] Nevertheless, this membrane was discontinued and is no longer available.

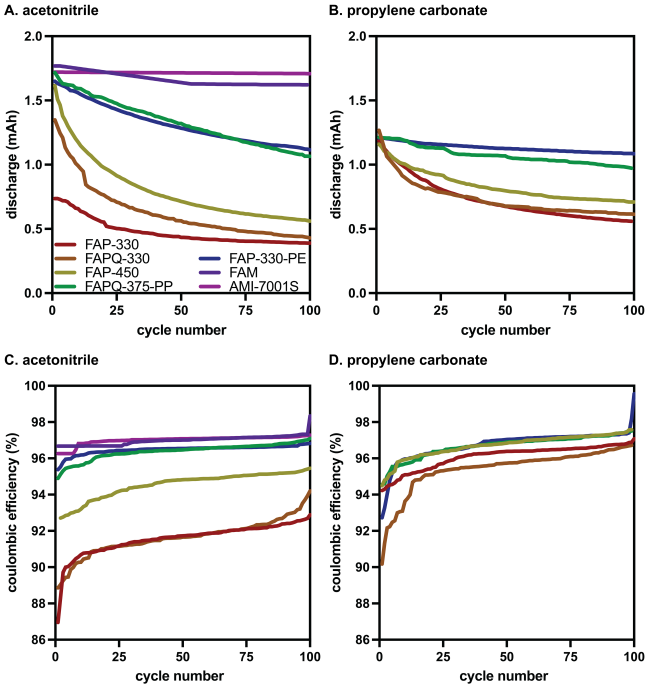

Figure 3. Capacity fade in MeCN (A) and in PC (B). Coulombic efficiency in MeCN (C) and in PC (D) over 100 cycles. The theoretical capacity of the battery is 2.7 mAh.

Table 2. Dry thickness, ionic conductivity, and voltage efficiency values for AEMs in MeCN and PC.

AEM	dry thickness (μm)	MeCN	PC	MeCN	PC
		PF_6^- ion conductivity (mS/cm)		voltage efficiency (%)	
FAP-330	32	18 ± 2	9.4 ± 0.5	87 ± 1	80 ± 1
FAPQ-330	36	22 ± 3	8.4 ± 0.4	90 ± 1	74 ± 1
FAP-450	56	11 ± 1	4.9 ± 0.3	95 ± 1	78 ± 1
FAPQ-375-PP	107	3.9 ± 0.2	0.69 ± 0.01	90 ± 1	34 ± 1
FAP-330-PE	45	18 ± 2	5.6 ± 0.2	95 ± 1	66 ± 1
FAM	526	0.0049 ± 0.0002	0.0002 ± 0.0001	21.0 ± 0.5	n.d.
AMI-7001S	568	0.0273 ± 0.0007	0.0002 ± 0.0001	33.5 ± 0.5	n.d.

Many factors compete in optimizing RFBs. A membrane with a large thickness may have little to no crossover but if it does not effectively allow the passage of supporting electrolyte ions, the voltage efficiency will be low. Indeed, the membranes that performed best in crossover studies, such as FAM and AMI-7001S in MeCN, were the worst performers in a flow battery due to low voltage efficiency. Alternatively, a lower cell resistance oftentimes is a result of a thinner membrane, which in turn may have a fast crossover rate.

A standardized protocol is necessary to compare between commercial and synthesized membranes. If all studies use the same redox-active molecules, solvents, and supporting electrolytes for crossover and battery testing, a direct comparison can be made between different membranes. To this end, we recommend that all NARFB groups that are synthesizing their own AEMs use the following protocol as a baseline: solvent testing in MeCN, PC, DMF, DMA, and DME, crossover studies using Fc, $FcNPF_6$, and $BuV2PF_6$, implementation in a flow battery, and EIS to determine ionic conductivity. To maximize ionic conductivity of supporting electrolyte (e.g., KPF_6), we suggest using MeCN as a solvent over PC, assuming similar redox-active molecule solubility in both solvents. KPF_6 is a convenient supporting electrolyte because it has no ^1H or ^{13}C signals via nuclear magnetic resonance spectroscopy (NMR), simplifying spectral analysis, which may be used to monitor redox-active molecule degradation. Subsequent battery testing should support the initial crossover rates observed in the H-cell and will provide a perspective on the long-term use of membranes. If this protocol is widely adopted, it will be easier to benchmark membranes and push the boundaries of membrane fabrication for RFBs.

Limitations and other considerations. Our workflow focuses on the membranes, and an easily translatable performance test to benchmark them. However, some conditions must be considered when adopting our methodology. Although Fc, $FcNPF_6$, and $BuV2PF_6$ are good model compounds, we recognize that crossover can also be mitigated through chemical synthesis (i.e., installing ionic functional groups onto redox molecules to be repelled by ion exchange membranes), meaning that our measured crossover rates of neutral, 1^+, and 2^+ species may not translate perfectly to other molecules. Additionally, some membrane characterization methods (i.e., ion-exchange capacity[54], swelling/sorption with different supporting electrolytes[55], and surface area/pore size of the membrane[56]) lie beyond the scope of this study but are important for full characterization of new membranes. Other methods to evaluate electrochemical performance and crossover *in situ* include dialysis diagnostics by Darling and coworkers, using an applied electric field[57] and compositionally unbalanced symmetric cell cycling by Brushett and coworkers.[58] Furthermore, our protocol is performed at low concentrations but transport and membrane properties (i.e., conductivity, partitioning, swelling) are likely to change at application-relevant active species concentrations.[59] Battery performance depends on volume, flow rate, concentrations of redox species, viscosity, electrode area, temperature, battery cell structure, and many other parameters. With these considerations, we emphasize that this study is for membrane comparison, and the relative values between the model compounds and membranes are what enable a precise comparison.

CONCLUSIONS

Commercially available AEMs were examined as potential membranes for NARFBs. Performance was compared based on structural stability in nonaqueous solvents, ionic conductivity of the charge carrying ion, crossover of the redox-active molecules, and a 100-cycle flow battery. Of the 26 membranes initially tested, only seven membranes emerged as good candidates for full evaluation. Overall, no commercial anion exchange membrane studied had an acceptable performance in *all* categories. Based on our data, FAPQ-375-PP and FAP-330-PE are the best membrane candidates for nonaqueous redox flow batteries in acetonitrile and only FAP-330-PE works well in propylene carbonate; however, these two membranes have been discontinued by the manufacturer. Consequently, new membranes (commercial or synthesized[60,61,62,63]) are needed for NARFBs and should be evaluated using our suggested protocol to accurately benchmark them against existing membranes.

ASSOCIATED CONTENT

Supporting Information

All materials, synthetic and electrochemical procedures, structural (NMR, MS, and elemental analysis) and electrochemical characterization (crossover, CV, EIS, batteries), solvent uptake and swelling studies, and photos of all AEMs in organic solvents are provided in the supporting information. (PDF)

The Supporting Information is available free of charge on the ACS Publications website.

AUTHOR INFORMATION

Corresponding Author

*Anne J. McNeil – Department of Chemistry and Macromolecular Science and Engineering Program, University of Michigan, Ann Arbor, Michigan 48109-1055, United States; orcid.org/0000-0003-4591-3308; Email: ajmcneil@umich.edu

*Shelley D. Minteer – Department of Chemistry, Missouri University of Science and Technology, Rolla, Missouri, 65409-6518, United States; orcid.org/0000-0002-5788-2249; Email: shelley.minteer@mst.edu

ORCID

Jessica L. Tami 0000-0003-3106-5790

Motiur Mazumder 0000-0002-3095-3019

Anne J. McNeil 0000-0003-4591-3308

Shelley D. Minteer 0000-0002-5788-2249

Author Contributions

CRediT: **Jessica L. Tami** contributed to conceptualization (equal), data curation (equal), formal analysis (equal), methodology (equal), visualization (lead), writing original draft (lead), and writing review & editing (lead). **Md. Motiur R. Mazumder** contributed to conceptualization (equal), data curation (equal), formal analysis (equal), and methodology (equal). **Grace E. Cook** contributed to data curation and methodology. **Shelley D. Minteer** contributed to conceptualization, funding acquisition, investigation, project administration, resources, supervision, and writing review & editing. **Anne J. McNeil** contributed to conceptualization, funding acquisition, investigation, project administration, resources, supervision, and writing review & editing.

Funding Sources

This research was supported by the Department of Energy through the Joint Center for Energy Storage Research (JCESR), an Energy Innovation Hub funded by the U.S. Department of Energy, Office of Science, Basic Energy Sciences.

ACKNOWLEDGMENT

J.L.T., M.M.R.M., A.J.M. and S.D.M. gratefully acknowledge support and helpful conversations from the Joint Center for Energy Storage Research.

ABBREVIATIONS

AEM, anion exchange membrane; Fc, ferrocene; RFB, redox flow battery; NARFB, nonaqueous redox flow battery; MeCN, acetonitrile; PC, propylene carbonate; DMF, *N,N*-dimethylformamide; DMA, *N,N*-dimethylacetamide; DME, dimethoxyethane; ASR, area specific resistance; NMR, nuclear magnetic resonance spectroscopy; UV-Vis, ultraviolet-Visible spectroscopy; OCV, open circuit voltage.

REFERENCES

[1]Ziegler, M. S.; Mueller, J. M.; Pereira, G. D.; Song, J.; Ferrara, M.; Chiang, Y.-M.; Trancik, J. E. *Joule* **2019**, *3*, 2134–2153.
[2]Sánchez-Díez, E.; Ventosa, E.; Guarnieri, M.; Trovò, A.; Flox, C.; Marcilla, R.; Soavi, F.; Mazur, P.; Aranzabe, E.; Ferret, R. *J. Power Sources* **2021**, *481*, 228804.
[3]Noack, J.; Roznyatovskaya, N.; Herr, T.; Fischer, P. *Angew. Chem. Int. Ed.* **2015**, *54*, 9776–9809.
[4]Arévalo-Cid, P.; Dias, P.; Mendes, A.; Azevedo, J. *Sustainable Energy Fuels* **2021**, *5*, 5366–5419.
[5]Choi, C.; Kim, S.; Kim, R.; Choi, Y.; Kim, S.; Jung, H.; Yang, J. H.; Kim, H.-T. *Renew. Sustain. Energy Rev.* **2017**, *69*, 263–274.
[6]Lourenssen, K.; Williams, J.; Ahmadpour, F.; Clemmer, R.; Tasnim, S. *J. Energy Storage* **2019**, *25*, 100844.
[7]Cunha, Á.; Martins, J.; Rodrigues, N.; Brito, F. P. *Int. J. Energy Res.* **2014**, *39*, 889–918.
[8]Kühnel, R.-S.; Reber, D.; Battaglia, C. *J. Electrochem. Soc.* **2020**, *167*, 070544.
[9]Li, M.; Rhodes, Z.; Cabrera-Pardo, J.; Minteer, S. D. *Sustain. Energy Fuels* **2020**, *4*, 4370–4389.
[10]Huang, Y.; Gu, S.; Yan, Y.; Fong Yau Li, S. *Curr. Opin. Chem. Eng.* **2015**, *8*, 105–113.
[11]Yuan, J.; Pan, Z. -Z.; Jin, Y.; Qui, Q.; Zhang, C.; Zhao, Y.; Li, Y. *J. Power Sources* **2021**, *500*, 229983.
[12]Hendriks, K. H.; Robinson, S. G.; Braten, M. N.; Sevov, C. S.; Helms, B. A.; Sigman, M. S.; Minteer, S. D.; Sanford, M. S. *ACS Cent. Sci.* **2018**, *4*, 189–196.
[13]Doris, S. E.; Ward, A. L.; Baskin, A.; Frischmann, P. D.; Gavvalapalli, N.; Chénard, E.; Sevov, C. S.; Prendergast, D.; Moore, J. S.; Helms, B. A. *Angew. Chem. Int. Ed.* **2017**, *56*, 1595–1599.
[14]De La Garza, G. D.; Preet Kaur, A.; Shkrob, I. A.; Robertson, L. A.; Odom, S. A.; McNeil, A. J. *J. Mat. Chem. A*, **2022**, *10*, 18745–18752.
[15]Kim, D.; Sanford, M. S.; Vaid, T. P.; McNeil, A. J. *Chem. Eur. J.* **2022**, *28*, e202200149.
[16]Nagarjuna, G.; Hui, J.; Cheng, K. J.; Lichtenstein, T.; Shen, M.; Moore, J. S.; Rodríguez-López, J. *J. Am. Chem. Soc.* **2014**, *136*, 16309–16316.
[17]Duan, W.; Huang, J.; Kowalski, J. A.; Shkrob, I. A.; Vijayakumar, M.; Walter, E.; Pan, B.; Yang, Z.; Milshtein, J. D.; Li, B.; Liao, C.; Zhang, Z.; Wang, W.; Liu, J.; Moore, J. S.; Brushett, F. R.; Zhang, L.; Wei, X. *ACS Energy Lett.* **2017**, *2*, 1156–1161.
[18]Wei, X.; Duan, W.; Huang, J.; Zhang, L.; Li, B.; Reed, D.; Xu, W.; Sprenkle, V.; Wang, W. *ACS Energy Lett.* **2016**, *1*, 705–711.
[19]You, W.; Noonan, K. J. T.; Coates, G. W. *Prog. Polym. Sci.* **2020**, *100*, 101177.
[20]Zeng, L.; Zhao, T. S.; Wei, L.; Jiang, H. R.; Wu, M. C. *Appl. Energy* **2019**, *233–234*, 622–643.
[21]Du, N.; Roy, C.; Peach, R.; Turnbull, M.; Thiele, S.; Bock, C. *Chem. Rev.* **2022**, *122*, 11830–11895.
[22]Matsuda, Y.; Tanaka, K.; Okada, M.; Takasu, Y.; Morita, M.; Matsumura-Inoue, T. *J. Appl. Electrochem.* **1988**, *18*, 909–914.
[23]Liu, Q.; Sleightholme, A. E. S.; Shinkle, A. A.; Li, Y.; Thompson, L. T. *Electrochem. Comm.* **2009**, *11*, 2312–2315.
[24]Mun, J.; Lee, M.-J.; Park, J.-W.; Oh, D.-J.; Lee, D.-Y.; Doo, S.-G. *Electrochem. Solid-State Lett.* **2012**, *15*, A80.
[25]Shin, S.-H.; Yun, S.-H.; Moon, S.-H. *RSC Adv.* **2013**, *3*, 9095–9116.
[26]Robinson, S. G.; Yan, Y.; Hendricks, K. H.; Sanford, M. S.; Sigman, M. S. *J. Am. Chem. Soc.* **2019**, *141*, 10171–10176.
[27]Shrestha, A.; Hendricks, K. H.; Sigman, M. S.; Minteer, S. D.; Sanford, M. S. *Chem. Eur. J.* **2020**, *26*, 5369–5373.
[28]Yan, Y.; Robinson, S. G.; Sigman, M. S.; Sanford, M. S. *J. Am. Chem. Soc.* **2019**, *141*, 15301–15306.
[29]Montoto, E. C.; Nagarjuna, G.; Moore, J. S.; Rodríguez-López, J. *J. Electrochem. Soc.* **2017**, *164*, A1688.
[30]Yan, Y.; Situala, P.; Odom, S. A.; Vaid, T. P. *ACS Appl. Mater. Interfaces* **2022**, *14*, 49633–49640.
[31]Ahn, S.; Jang, H. H.; Kang, J.; Na, M.; Seo, J.; Singh, V.; Joo, J. M.; Byon, H. R. *ACS Energy Lett.* **2021**, *6*, 3390–3397.
[32]Daub, N.; Hendricks, K. H.; Janssen, R. A. J. *Batteries & Supercaps* **2022**, *5*, e202200386.
[33]Krivina, R. A.; Lindquist, G. A.; Yang, M. C.; Cook, A. K.; Hendon, C. H.; Motz, A. R.; Capuano, C.; Ayers, K. E.; Hutchinson, J. E.; Boettcher, S. W. *ACS Appl. Mater. Interfaces* **2022**, *14*, 18261–18274.
[34]Hudak, N. S.; Small, L. J.; Pratt, H. D.; Anderson, T. M. *J. Electrochem. Soc.* **2015**, *10*, A2188–A2194.
[35]Liang, Z.; Attanayake, N. H.; Greco, K. V.; Neyhouse, B. J.; Barton, J. L.; Kaur, A. P.; Eubanks, W. L.; Brushett, F. R.; Landon, J.; Odom, S. A. *ACS Appl. Energy Mater.* **2021**, *4*, 5443–5451.
[36]Mushtaq, K.; Lagarteria, T.; Zaidi, A. A.; Mendes, A. *J. Energy Storage* **2021**, *40*, 102713.
[37]George, T. Y.; Thomas, I. C.; Haya, N. O.; Deneen, J. P.; Wang, C.; Aziz, M. J. *ACS Appl. Mater. Interfaces* **2023**, *15*, 57252–57264.

[38]Cassady, H. J.; Yang, Z.; Rochow, M. F.; Saraidaridis, J. D.; Hickner, M. A. *J. Electrochem. Soc.*, **2024**, *171*, 030527.
[39]Lehmann, M. L.; Tyler, L.; Self, E. C.; Yang, G.; Nanda, J.; Saito, T. *Chem* **2022**, *8*, 1611–1636.
[40]Gong, K.; Fang, Q.; Gu, S.; Li, S. F. Y.; Yan, Y. *Energy Environ. Sci.* **2015**, *8*, 3515–3530.
[41]Alder, C. M.; Hayler, J. D.; Henderson, R. K.; Redman, A. M.; Shukla, L.; Shuster, L. E.; Sneddon, H. F. *Green chem.* **2016**, *18*, 3879–3890.
[42] The hydrodynamic radii are approximated with the Stokes-Einstein equation, wherein the radius is inversely proportional to the diffusion coefficient of the molecule in solution (diffusion coefficients are calculated in SI Table S8) and solution viscosity, which is primarily affected by the solvent and excess supporting electrolyte. See ref: Berkowicz, S.; Perakis, F. *Phys. Chem. Chem. Phys.* **2021**, *23*, 25490.
[43]Li, M.; Odom, S. A.; Pancoast, A. R.; Robertson, L. A.; Vaid, T. P.; Agarwal, G.; Doan, H. A.; Wang, Y.; Suduwella, T. M.; Bheemireddy, S. R.; Ewoldt, R. H.; Assary, R. S.; Zhang, L.; Sigman, M. S.; Minteer, S. D. *ACS Energy Lett.* **2021**, *6*, 3932–3943.
[44]Gandomi, Y. A.; Aaron, D. S.; Houser, J. R.; Daugherty, M. C.; Clement, J. T.; Pezeshki, A. M.; Ertugrul, T. Y.; Moseley, D. P.; Mench, M. M. *J. Electrochem. Soc.* **2018**, *165*, A970.
[45]Adams & Chittenden Scientific Glass Coop Home Page. https://adamschittenden.com/ (accessed 2024/02/09).
[46] A. J. Bard and L. R. Faulkner, Electrochemical Methods: Fundamentals and Applications; Harris, D.; Swain, E.; Robey C.; Aiello, E., John Wiley and Sons, INC.: US, 2001; pp. 230–243.
[47]Wang, H.; Sayed, S. Y.; Luber, E. J.; Olsen, B. C.; Shirurkar, S. M.; Venkatakrishnan, S.; Tefashe, U. M.; Farquhar, A. K.; Smotkin, E. S.; McCreery, R. L.; Buriak, J. M. *ACS Nano* **2020**, *14*, 2575–2584.
[48]Yang, Z.; Tong, L.; Tabor, D. P.; Beh, E. S.; Goulet, M.-A.; De Porcellinis, D.; Aspuru-Guzik, A.; Gordon, R. G.; Aziz, M. J. *Adv. Energy Mater.* **2018**, *8*, 1702056.
[49]Díaz, J. C.; Kitto, D.; Kamcev, J. *J. Membr. Sci.* **2023**, *669*, 121304.
[50]Su, L.; Darling, R. M.; Gallager, K. G.; Xie, W.; Thelen, J. L.; Badel, A. F.; Barton, J. L.; Cheng, K. J.; Balsara, N. P.; Moore, J. S.; Brushett, F. R. *J. Electrochem. Soc.* **2016**, *163*, A5253.
[51]Darling, R.; Gallaher, K.; Xie, W.; Su, L.; Brushett, F. *J. Electrochem. Soc.* **2016**, *163*, A5029.
[52]Kong, T.; Li, J.; Wang, W.; Zhou, X.; Xie, Y.; Ma, J.; Li, X.; Wang, Y. *ACS Appl. Mater. Interfaces* **2024**, *16*, 752–760.
[53]Modak, S. V.; Shen, W.; Singh, S.; Herrera, D.; Oudeif, F.; Goldsmith, B. R.; Huan, X.; Kwabi, D. G. *Nat. Commun.* **2023**, *14*, 3602.
[54]Jacquemond, R. R.; Geveling, R.; Forner-Cuenca, A.; Nijmeijer, K. *J. Electrochem. Soc.* **2022**, *169*, 080528.
[55]Geise, G. M.; Paul, D. R.; Freeman, B. D. *Prog. Polym. Sci.* **2014**, *39*, 1–42.
[56]Machado, C. A.; Brown, G. O.; Yang, R.; Hopkins, T. E.; Pribyl, J. G.; Epps, T. H. *ACS Energy Lett.* **2021**, *6*, 158–176.
[57]Darling, R. M.; Saraidaridis, J. D.; Shovlin, C.; Fortin, M. *J. Electrochem. Soc.* **2022**, *169*, 030514.
[58]Neyhouse, B. J.; Darling, R. M.; Saraidaridis, J. D.; Brushett, F. R. *J. Electrochem. Soc.* **2023**, *170*, 080514.
[59]Fenton, Jr., A. M.; Kant Jha, R.; Neyhouse, B. J.; Preet Kaur, A.; Dailey, D. A.; Odom, S. A.; Brushett, F. R. *J. Mater. Chem. A* **2022**, *10*, 17988.
[60]Peltier, C. R.; Rhodes, Z.; Macbeth, A. J.; Milam, A.; Carroll, E.; Coates, G. W.; Minteer, S. D. *ACS Energy Lett.* **2022**, *7*, 4118–4128.
[61]Mazumder, M. R.; Jadhav, R. G.; Minteer, S. D. *ACS Mater. Au* **2023**, *3*, 557–568.
[62]Li, Y.; Sniekers, J.; Malaquias, J.C.; Van Goethem, C.; Binnemans, K.; Fransaer, J.; Vankelecom, I. F. J. *J. Power Sources* **2018**, *378*, 338–344.
[63]Mandal, M.; Huang, G.; Hassan, N. U.; Mustain, W. E.; Kohl, P. A. *J. Mater. Chem A* **2020**, *8*, 17568–17578.